From periodic travelling waves to travelling fronts in the spike-diffuse-spike model of dendritic waves

S Coombes

Nonlinear and Complex Systems Group, Department of Mathematical Sciences, Loughborough University, Loughborough, Leicestershire, LE11 3TU, UK.

Abstract

In the vertebrate brain excitatory synaptic contacts typically occur on the tiny evaginations of neuron dendritic surface known as dendritic spines. There is clear evidence that spine heads are endowed with voltage dependent excitable channels and that action potentials invade spines. Computational models are being increasingly used to gain insight into the functional significance for a spine with excitable membrane. The spike-diffuse-spike (SDS) model is one such model that admits to a relatively straightforward mathematical analysis. In this paper we demonstrate that not only can the SDS model support solitary travelling pulses, already observed numerically in more detailed biophysical models, but that it has periodic travelling wave solutions. The exact mathematical treatment of periodic travelling waves in the SDS model is used, within a kinematic framework, to predict the existence of connections between two periodic spike trains of different interspike interval. The associated wave front in the sequence of interspike intervals travels with a constant velocity without degradation of shape, and might therefore be used for robust encoding of information.

keywords dendritic spines, travelling waves, integrate-and-fire

1 Introduction

Dendritic spines are small mushroom like appendages found on the dendrites of neurons in the central nervous system of taxa as divergent as bees and humans [1]. A dendritic spine has a general appearance consistent with a bulbous head (with surface area of order $1\mu m^2$) and a tenuous stem (of length

[1] S.Coombes@lboro.ac.uk

around 1μm). They are particularly abundant (between $100,000$ and $300,000$) in single cortical pyramidal cells. In parts of the mammalian nervous system, the most common way a synapse is formed between two nerve cells is by the presynaptic component making contact with a dendritic spine [2]. Since their identification in 1911 by Ramón y Cajál, with the use of Golgi staining, there has been much discussion as to whether the spine simply serves as a site for synaptic input or whether the spine itself contributes to information processing. Recent studies using electron microscopy and fluorescence imaging are beginning to clarify matters (see Segev and Rall [3] for a recent discussion). For example, there is now overwhelming experimental evidence for excitable channels and for action potentials in dendrites [4]. Calcium imaging experiments have also been used to show that calcium channels exist in spine heads and are associated with the generation of spine head action potentials [5]. Such experiments support the notion that spines can act to boost and/or modify the input coming from the distal dendrite into the soma of a neuron. A good example is the many dendritic spines found on cerebellar Purkinje cells. These spines receive their input from parallel fibers of the granule cells and act in concert to bring about action potentials in the Purkinje cells. Other studies have shown that dendritic spines are dynamic structures, sensitive to environmental factors, whose physical, chemical and electrical characteristics change over time [6]. Experimental evidence is also growing that spines are intimately involved in neuronal plasticity and learning (see Harris and Kater [7] for a review). However, their small size means that contemporary electrophysiology and biochemical techniques cannot accurately measure the activity of single spines. This, in part, has encouraged the development of computational models based upon experimentally accessible information [8–10]. Computational models are useful for gaining insight into the functional significance of spines, and in particular the way in which spines modulate synaptic efficacy [11]. Theoretical studies have addressed the role of voltage dependent channels for spine plasticity [12–14] and demonstrated that individual spines can amplify synaptic input by firing an action potential [12]. Rall and Rinzel [15] were perhaps the first to propose that spine stem resistance could act as a tunable synaptic weight parameter. The potentially high input impedance of spines means that they are ideal candidates for influencing the temporal filtering properties of neurons and that they may play an important role in the decoding of neuronal information [16]. Unfortunately, physiological evidence regarding the role of spines in actual information processing is lacking [1]. One of the more appropriate computational models for assessing the information processing abilities of a dendritic system with spines is that developed by Baer and Rinzel [17]. Indeed numerical simulations of this model have shown that global signals, in the form of travelling solitary pulses, may propagate in a passive cable structure coupled to excitable spines.

In this paper we focus on global signals that may be supported in dendritic systems with active spines, with the emphasis on the response of such systems

to spike train input. In section 2 we describe the model of Baer and Rinzel and illustrate the typical response of this system to periodic and non-periodic spike train input, at a specific synaptic location, using numerical simulations. In the former case periodic travelling waves are observed for a wide range of system parameters. For inputs with a step change in the interspike interval (ISI) of the applied signal a steady spike train with a smooth transition region is observed. Interestingly, after some transient behavior, the transition region propagates with constant speed and without loss of shape. This suggests that, for the Baer and Rinzel model of dendritic tissue with active spines, signals encoded in spike trains may be transmitted without degradation. This numerical observation motivates the rest of the paper which presents a mathematical study of such phenomenon. The complexity of the Baer and Rinzel model precludes a straightforward mathematical analysis, which is why we turn to the recently introduced spike-diffuse-spike (SDS) model [18]. The SDS model is an idealized system for the description of dendritic wave propagation in spine studded dendritic trees, highlighting space and time scales over detailed mechanisms. The SDS model has already been shown to support travelling solitary waves, whose properties are in accord with those originally observed numerically by Baer and Rinzel [18]. In section 3 we formulate periodic travelling wave solutions of the SDS model. The analytical tractability of the model allows the calculation of the dispersion relationship for the system, giving the speed of solution as a function of its period. As a consequence of the refractoriness of the spine head dynamics in the SDS model the dispersion curve has an exponential shape. In section 4 we develop a kinematic theory of spike trains in the SDS model based around the dispersion curve for periodic travelling waves. This allows us to study the dynamics of non-periodic waves, including those generated in response to an external signal in the form of a spike train. For the exponential shape of the SDS dispersion curve derived in section 3 we show analytically the existence of connections between periodic orbits (with differing ISIs). These solutions describe precisely the type of propagating front observed numerically in the Baer and Rinzel model when the external input is in the form of a spike train with a step change in the interspike interval. The stability of solutions is also analyzed within the kinematic framework and shown to be dependent on the derivative of the dispersion relationship. Finally, in section 5, we present a discussion of the work in this paper.

2 Travelling fronts in the Baer and Rinzel model

In order to analyze the interactions between spines, Baer and Rinzel formulated a type of cable theory in which the distribution of spines is treated as a continuum. The formulation retains the notion that there is no direct electrical coupling between neighboring spines. Voltage spread along a uniform

passive cable is the only way for the spines to interact; spines are electrically independent from one another. Active membrane in the spine-head is modeled by Hodgkin-Huxley kinetics. The density of spines, the spine stem current and the membrane potential in spine heads are considered as distributed variables. The continuum model of Baer and Rinzel, with spine density per unit area of dendritic membrane $\rho(x)$ at location x is given by

$$C\frac{\partial V}{\partial t} = -g_L(V - V_L) + \frac{1}{r_a \pi d}\frac{\partial^2 V}{\partial x^2} + \rho(x)\frac{\widehat{V} - V}{r} \tag{1}$$

$$\widehat{C}\frac{\partial \widehat{V}}{\partial t} = -I(\widehat{V}, m, n, h) - \frac{\widehat{V} - V}{r} + I(x, t) \tag{2}$$

Equation (1) describes the dynamics of an infinite uniform passive cable of diameter d with voltage $V(x,t)$ such that the term $\rho[\widehat{V} - V]/r$ describes the flow of current between the cable shaft and the spine-head above the shaft via the ohmic spine-stem resistance of strength r. The terms V_L and g_L are respectively a constant leakage reversal potential and a leakage conductance per unit area of membrane. The parameter r_a represents the intracellular resistance per unit length of the cable. The electronic length constant λ is given by $\lambda^2 = 1/(\pi d r_a g_L)$ and the membrane time constant (of the dendritic cable) by $\tau = C/g_L$. For the rest of our discussion we consider the case that the spine density function is a constant $\rho(x) = \rho$. The excitable dynamics of the voltage in the spine-head $\widehat{V}(x,t)$ is driven by the flow of current from the shaft to the spine and is described with equation (2). Any externally injected current is described with the term $I(x,t)$ in (2). From now on we choose specific membrane capacitances C and $\widehat{C}$ such that $C = \widehat{C}$ and take $C = 1$ without loss of generality. It is also convenient to choose a length scale such that $r_a \pi d = 1$. The Hodgkin-Huxley dynamics, described with the use of the function $I(\widehat{V}, m, n, h)$, is a function of $\widehat{V}$ and three time and voltage dependent conductance variables m, n and h:

$$I(\widehat{V}, m, n, h) = g_K n^4(\widehat{V} - V_K) + g_{Na} h m^3(\widehat{V} - V_{Na}) + g_L(\widehat{V} - V_L) \tag{3}$$

where g_K, g_{Na} and g_L are constants and V_L, V_K and V_{Na} represent the constant membrane reversal potentials associated with the leakage, potassium and sodium channels respectively. For simplicity we take the currents due to the leakage terms in the model of the cable and those in the model of the spine-head to be identical. The conductance variables m, n and h take values between 0 and 1 and approach the asymptotic values $m_\infty(\widehat{V})$, $n_\infty(\widehat{V})$ and $h_\infty(\widehat{V})$ with time constants $\tau_m(\widehat{V})$, $\tau_n(\widehat{V})$ and $\tau_h(\widehat{V})$ respectively. Summarizing, we have that

$$\tau_X(\widehat{V})\frac{\mathrm{d}X}{\mathrm{d}t} = X_\infty(\widehat{V}) - X, \quad X \in \{m, n, h\} \tag{4}$$

The six functions $\tau_X(\widehat{V})$ and $X_\infty(\widehat{V})$, $X \in \{m, n, h\}$, are given in appendix A. Using numerical simulation, Baer and Rinzel have shown that the combination

of diffusion along the cable with input from electrotonically separated active spines can lead to the propagation of a solitary travelling wave. The speed of this travelling wave decreases as a function of the spine density [17,19]. Moreover, there is propagation failure for too large a spine-stem resistance or too small a spine density. We now extend the original investigations of Baer and Rinzel and consider the case that $I(x,t)$ represents a train of stimulus pulses added at a certain dendritic position. For numerical purposes we restrict attention to a finite cable of length L and stimulate at the point $x = 0$ so that we may write $I(x,t) = I(t)\delta(x)$. Using a spatial discretization (or compartmentalization) of the system with a forward difference scheme allows a simple numerical study of the Baer and Rinzel system. For N compartments we use a spatial step size $\Delta x = L/N$ and a temporal step size of $\Delta t = 1/4(\Delta x)^2$. We here denote a spike train by the sequence $T^n(x)$: the set of times at which the nth spike in the train passes at a position x on the cable. At $x = 0$ spike times are specified externally by $T^n(0)$, but for $x > 0$ we need to be more precise about the nature of a spike. We define the time at which the nth spike occurs at position x by introducing a threshold parameter $V_{\rm th}$ such that

$$T^n(x) = \inf\{t \mid \widehat{V}(x,t) \geq V_{\rm th}, \frac{\partial \widehat{V}(x,t)}{\partial t} > 0 \ ; \ t \geq T^{n-1}(x)\} \tag{5}$$

Interspike intervals are defined by $\Delta_n(x) = T^n(x) - T^{n-1}(x)$. A general rectangular stimulus train has the form $I(t) = \sum_n P(t - T^n(0))$ with $P(t) = I_0\Theta(t)\Theta(\tau_d - t)$, where I_0 is the magnitude of an applied pulse, τ_d its duration and $\Theta(x)$ is a step function with $\Theta(x) = 1$ for $x \geq 0$ and is zero otherwise. It is easily verified that the system can support periodic travelling waves in response to a periodic stimulus train. Throughout this section we take the threshold for spike initiation to be $V_{\rm th} = -30$mV. As the interspike interval between stimuli increases the speed of the resultant travelling wave approximates that of a single solitary travelling pulse. Rather than focus on the detailed properties of such waves we pursue the more interesting observation that the system supports *connections* between periodic orbits. These connections take the form of spike trains whose ISI for a fixed time and spatial location is a constant with period $\Delta_{(1)}$ and for some much later time takes a different constant value, say $\Delta_{(2)}$. For intermediate values of time the ISIs vary smoothly between $\Delta_{(1)}$ and $\Delta_{(2)}$. Solutions of this type are most easily observed by choosing $I(t)$ to have the form

$$I(t) = \sum_{n=0}^{n^*} P(t - n\Delta_{(1)}) + \sum_{n=n^*}^{\infty} P(t - n^*\Delta_{(1)} - (n - n^*)\Delta_{(2)}) \tag{6}$$

which describes a step sequence in the ISIs, between $\Delta_{(1)}$ and $\Delta_{(2)}$, occurring after n^* firing events at $x = 0$. An illustration of this signal is given in figure 1. In all direct simulations of the Baer and Rinzel model we take $I_0 = 35$ and $\tau_d = 2$. In figure 2 we show the results of a numerical simulation for the temporal evolution of the excitable spine head dynamics $\widehat{V}$ at a spatial position

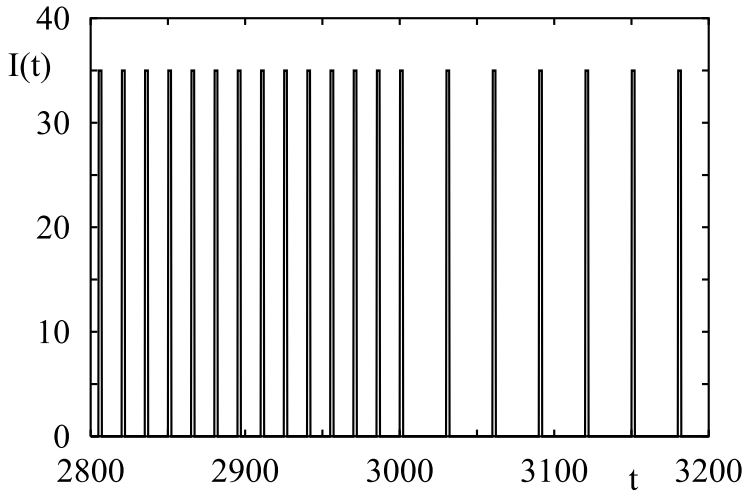

Fig. 1. An example of a stimulus signal $I(t)$ used to generate a smooth connection between orbits with differing ISIs. In this case we use equation (6) with $I_0 = 35$, $\tau_d = 2$, $\Delta_{(1)} = 15$, $\Delta_{(2)} = 30$ and $n^* = 200$.

of 3/4 along the length of the cable away from the point of stimulation. The spine head dynamics clearly makes a transition from spiking with period $\Delta_{(1)}$ to $\Delta_{(2)}$ as time increases. Figure 3 shows the corresponding behavior of the cable at the same spatial location. Once again one can clearly see a connection between periodic orbits, but with this time there is also a change in amplitude as well as frequency. Numerical simulations suggest that the smaller ISI always

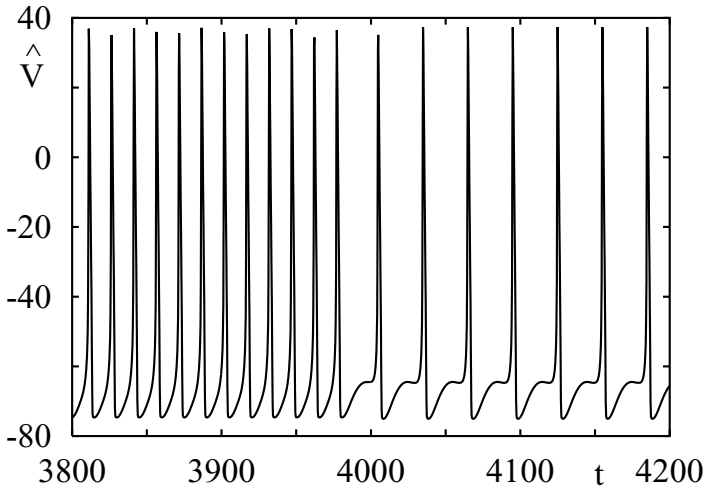

Fig. 2. Temporal evolution of spine head dynamics $\widehat{V}$ at position $3L/4$ along the cable, showing a connection between two different ISIs. $L = 200$, number of compartments used is 2000, $r = 1$, $\rho = 25$, $\Delta_{(1)} = 15$, $\Delta_{(2)} = 30$, $n^* = 200$.

corresponds to a lower maximum value of the action potential on the cable. In figure 4 we use an alternative way to view these connections to periodic orbits

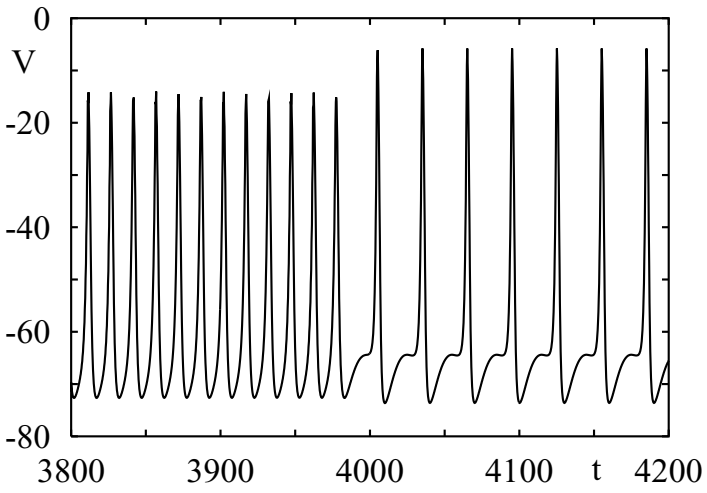

Fig. 3. Temporal evolution of cable dynamics V at position $3L/4$ along the cable, showing a connection between two different ISIs. Parameters as for figure 2.

by plotting the ISIs, at various positions along the cable, as a function of the number of firing events at those positions. An initial step sequence in the ISIs at $x = 0$ smoothes out before eventually propagating with an invariant shape and constant speed. The speed of the front in the ISIs should not be confused with the speed of the periodic travelling wave. Numerics also suggest that a

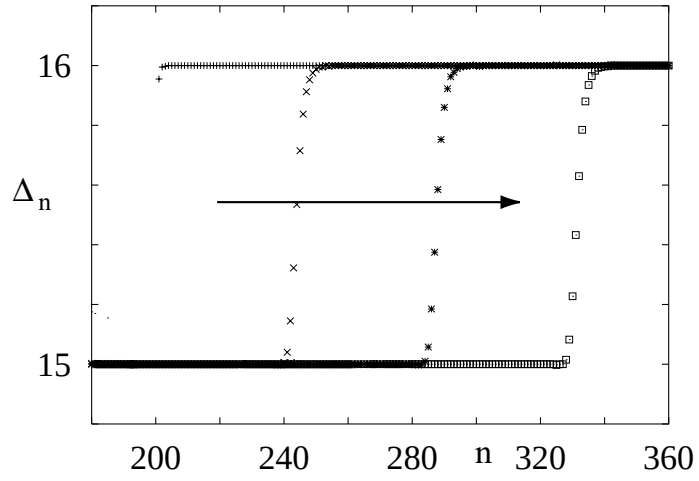

Fig. 4. An example of a connection between periodic orbits in the Baer and Rinzel model. Initial data is in the form of a spike train with a step change in the ISIs between $\Delta_{(1)} = 15$ and $\Delta_{(2)} = 16$. The initial data evolves to form a smooth connection between the periodic orbits (periodic spike trains with constant ISIs $\Delta_{(1)}$ and $\Delta_{(2)}$) that can then propagate in an invariant fashion with constant speed. $L = 200$, number of compartments used is 2000, $r = 1$, $\rho = 25$, $\Delta_{(1)} = 15$, $\Delta_{(2)} = 16$, $n^* = 200$. Data is shown at the following positions along the cable: 0, $L/4$, $L/2$ and $3L/4$ (the arrow indicates the data with increasing position).

step change in the ISIs is less smoothed and travels slower as the difference between $\Delta_{(1)}$ and $\Delta_{(2)}$ increases. An example of this is shown in figure 5. In

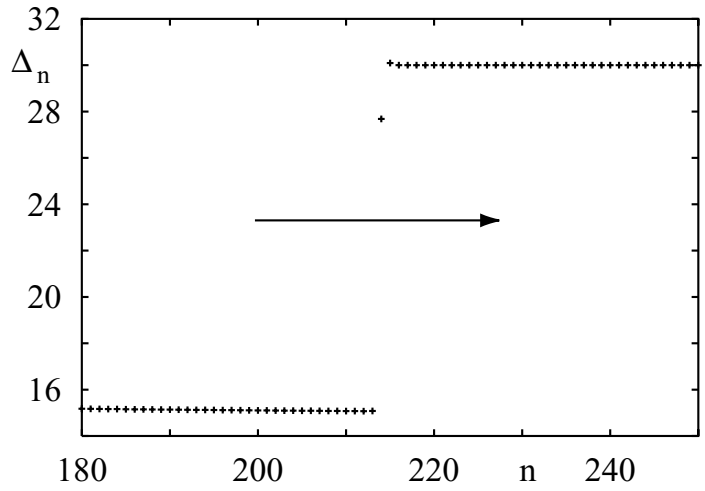

Fig. 5. Same parameters as in figure 4 with $\Delta_{(2)} = 30$. Data shown at a spatial position $3L/4$. In comparison to figure 4 (where $\Delta_{(1)}$ and $\Delta_{(2)}$ are closer) we see a steepening of the resultant wave front and a slower propagation velocity for the front.

the remainder of this paper we use a recent reduction of the Baer and Rinzel model, the so-called spike-diffuse-spike model [18], that admits to an exact mathematical treatment consistent with these numerical observations.

3 An exact treatment of periodic travelling waves in the spike-diffuse-spike model

An exact mathematical treatment of the Baer and Rinzel model is yet to be performed, due in part to its complexity. By replacing the model spine head dynamics with the FitzHugh-Nagumo (FHN) system and further ignoring the dynamics of the FHN refractory variable precise statements about travelling wave fronts have been made [19]. The inclusion of dynamics describing the refractory process complicates mathematical analysis. In order to make progress regarding the dynamics of solitary pulses, Coombes and Bressloff [18] formulated a reduction of the Baer and Rinzel model, the so-called spike-diffuse-spike (SDS) model, which retains many of its essential features. Moreover, the model supports travelling pulses whose calculated speed varies with system parameters as those observed numerically in the Baer and Rinzel. In both the SDS model and the original model of Baer and Rinzel a brief external input, say in the form of a synaptic current, leads to a spread of potential along a passive dendritic cable. The dynamics in the model spine head is driven

by this potential and for sufficiently large drive an action potential may be generated. There is then a large re-injection of current back into the dendrite that causes a further spread of potential along the cable so that the process is self-perpetuating. The major difference between the two models is the choice of excitable dynamics used for the description of the spine head. In the SDS model a simple integrate-and-fire (IF) process is chosen. Since such processes do not describe the evolution of an action potential, but instead flag the occurrence of one, the SDS model makes use of an explicit functional form for the action potential generated in the model spine head. After explaining the model in more mathematical terms we then determine the speed of periodic travelling waves analytically.

The continuum SDS model with spine density per unit area of dendritic membrane at location x given by $\rho(x)$, is expressed by the following equation:

$$\frac{\partial V}{\partial t} = -g_L V + \frac{\partial^2 V}{\partial x^2} + \rho(x)\frac{\widehat{V} - V}{r} \tag{7}$$

$$\widehat{V}(x,t) = \sum_{m\in\mathbb{Z}} \eta(t - T^m(x)) \tag{8}$$

Equation (7) describes the dynamics of an infinite uniform passive cable of fixed diameter with voltage $V(x,t)$ (relative to the reference level V_L used in the Baer and Rinzel model) coupled via an ohmic resistor to a spine head with voltage $\widehat{V}(x,t)$ (as in the original Baer and Rinzel model). In the SDS model the dynamics of the voltage in the spine-head $\widehat{V}(x,t)$ is driven by the flow of current from the shaft to the spine and is described with the aid of an integrate-and-fire mechanism [18]. The spine head dynamics is considered to be a sequence of pulses that are generated whenever the dynamics in the spine-head, driven by current from the shaft, crosses some threshold. The pulse-shape is chosen to mimic that of a real action potential, ie it has a biologically realistic magnitude and duration. The function $\eta(t)$ specifies the shape of an action potential and the firing times $T^m(x)$ are generated by an IF type firing mechanism:

$$T^n(x) = \inf\{t \mid U(x,t) \geq U_{\text{th}} \ ; \ t \geq T^{n-1}(x) + \tau_R\} \tag{9}$$

The term τ_R provides a simple model for the absolute refractory period of excitable spine head tissue. It is important to include such a delay in the SDS description since the IF process in the spine head does not have a refractory variable, such as effectively present in the Hodgkin-Huxley equations due to the behavior of the n and h gating variables. For $T^n(x) < t < T^{n+1}(x)$ the generator of the IF process, $U(x,t)$, evolves according to

$$\frac{\partial U}{\partial t} = -g_L U + \left[\frac{V - U}{r}\right] \tag{10}$$

subject to the reset condition $U(x,t^+) = U_{\text{re}}$ whenever $U(x,t) = U_{\text{th}}$. U_{th} is

recognized as the threshold for a firing event to occur whilst $U_{\rm re}$ represents the reset level of the IF process, with $U_{\rm re} < U_{\rm th}$. Without loss of generality we set $U_{\rm th} = 1$ and $U_{\rm re} = 0$. As for the discussion of section 2 we consider the case that the spine density function is a constant with $\rho(x) = \rho$ for all x.

We define a periodic travelling wave as one for which the firing times of the spine at $x \in \mathbb{R}$ satisfy $T^n(x) = (n+kx)\Delta$ for integer n. Here k is the wavenumber and $c = 1/(k\Delta)$ is the wave velocity. Hence, all spines fire at regular intervals Δ but at different times depending on their position along the cable. For a periodic travelling wave we have that

$$\widehat{V}(x,t) = F(t - x/c), \qquad F(t) = \sum_m \eta(t - m\Delta) \tag{11}$$

where $F(t)$ is periodic in Δ. We look for periodic travelling waves in the cable by assuming $V(x,t) = V(\xi)$, where $\xi = t - x/c$. From (7) periodic waves satisfy the following ordinary differential equation

$$k^2\Delta^2 V_{\xi\xi} - V_\xi - \epsilon V = -\frac{\rho}{r}\widehat{V} \tag{12}$$

where $V_\xi \equiv \mathrm{d}V/\mathrm{d}\xi$, $\epsilon = g_L + \rho/r$. For the simple choice of a rectangular pulse of duration equal in value to the refractory period

$$\eta(t) = \eta_0 \Theta(t)\Theta(\tau_R - t) \tag{13}$$

we have that $\widehat{V}(\xi) = \widehat{V}(\xi + \Delta)$, where

$$\widehat{V}(\xi) = \begin{cases} \eta_0 & 0 < \xi < \tau_R \\ 0 & \tau_R < \xi < \Delta \end{cases} \tag{14}$$

Solutions to (12) have the general form

$$V(\xi) = \begin{cases} \alpha_1 \mathrm{e}^{\lambda_+\xi} + \alpha_2 \mathrm{e}^{\lambda_-\xi} + \rho\eta_0/(\epsilon r) & 0 < \xi < \tau_R \\ \alpha_3 \mathrm{e}^{\lambda_+\xi} + \alpha_4 \mathrm{e}^{\lambda_-\xi} & \tau_R < \xi < \Delta \end{cases} \tag{15}$$

where $\lambda_\pm$ are given by

$$\lambda_\pm = \frac{1 \pm \sqrt{1 + 4\epsilon k^2\Delta^2}}{2k^2\Delta^2} \tag{16}$$

By demanding periodicity of the solution, continuity of the solution and continuity of its derivative we have four conditions that may be used to solve for the unknowns $\alpha_1 \ldots \alpha_4$. The solution to this system takes the form

$$\begin{aligned} \alpha_1 &= \sigma\lambda_- \frac{(1 - \mathrm{e}^{\lambda_+(\Delta - \tau_R)})}{(\mathrm{e}^{\lambda_+\Delta} - 1)} & \alpha_2 &= -\sigma\lambda_+ \frac{(1 - \mathrm{e}^{\lambda_-(\Delta - \tau_R)})}{(\mathrm{e}^{\lambda_-\Delta} - 1)} \\ \alpha_3 &= \sigma\lambda_- \frac{(1 - \mathrm{e}^{-\lambda_+\tau_R})}{(\mathrm{e}^{\lambda_+\Delta} - 1)} & \alpha_4 &= -\sigma\lambda_+ \frac{(1 - \mathrm{e}^{-\lambda_-\tau_R})}{(\mathrm{e}^{\lambda_-\Delta} - 1)} \end{aligned} \tag{17}$$

where

$$\sigma = \frac{\rho\eta_0}{\epsilon r(\lambda_- - \lambda_+)} \tag{18}$$

As yet the speed of the periodic travelling wave is still undetermined. We determine the speed of the wave in a self-consistent manner by demanding that the IF process in the spine head at position x reach threshold at times $T^n(x)$. The ordinary differential equation describing the dynamics in the spine head is given by

$$U_\xi = -\widehat{\epsilon}U + \frac{V}{r}, \qquad \widehat{\epsilon} = g_L + \frac{1}{r} \tag{19}$$

Integrating (19) and making use of the reset condition gives

$$1 = \mathrm{e}^{-\widehat{\epsilon}\Delta} \int_{\tau_R}^{\Delta} \mathrm{e}^{\widehat{\epsilon}\xi} \frac{V(\xi)}{r} \mathrm{d}\xi \tag{20}$$

Since $V(\xi)$ is given in terms of the undetermined parameter c, equation (21) defines a dispersion relation, $c = c(\Delta)$, for the speed of the wave as a function of the period Δ. Hence, the speed of a periodic travelling wave in the SDS model is completely determined by the equation

$$1 = \frac{1}{r}\left\{ \alpha_3 \frac{\mathrm{e}^{\lambda_+\Delta} - \mathrm{e}^{\widehat{\epsilon}(\tau_R-\Delta)}\,\mathrm{e}^{\lambda_+\tau_R}}{\widehat{\epsilon}+\lambda_+} + \alpha_4 \frac{\mathrm{e}^{\lambda_-\Delta} - \mathrm{e}^{\widehat{\epsilon}(\tau_R-\Delta)}\,\mathrm{e}^{\lambda_-\tau_R}}{\widehat{\epsilon}+\lambda_-} \right\} \tag{21}$$

This is an implicit formula for the speed of the travelling wave as a function of the period, for fixed parameter values r, ρ, τ_R, η_0 and g_L. For fixed realistic values of τ_R, η_0 and g_L the dispersion curve $c = c(\Delta)$ is parameterised by the spine stem resistance r and spine density ρ. Typically one finds that periodic solutions can only exist for sufficiently large values of ρ and sufficiently small values of r. As an illustration of this point we consider solutions of large period ($\Delta \to \infty$) in figure 6 and plot the locus of points in (r, ρ) parameter space where solutions to (21) cease to exist. In practice dispersion curves may be constructed numerically by writing equation (21) in the form $H(c, \Delta) = 0$ and using a numerical scheme to plot the zero contour of the two variable function $H(c, \Delta)$. The accuracy of the dispersion curve is then limited by the way that the contour is constructed. In the regime where periodic waves exist dispersion curves have a common structure for a range of r and ρ values. An example is given in figure 7 (using bsplines to fit the contour and for later convenience we plot $c^{-1}(\Delta)$ rather than $c(\Delta)$) where one can see that periodic travelling waves with periods smaller than that of the absolute refractory period τ_R cannot exist. Propagation of periodic travelling waves is blocked by a standing wave of zero speed as $\Delta \to \tau_R$ from above. Note also that, compared to the speed of the large period wave there is a slight increase in speed over a range of intermediate periods. Such a phenomenon has also been observed in dispersion curves of the Hodgkin-Huxley model of nerve fiber and is associated with waves of *supernormal* speed [20]. It would seem that to accommodate an

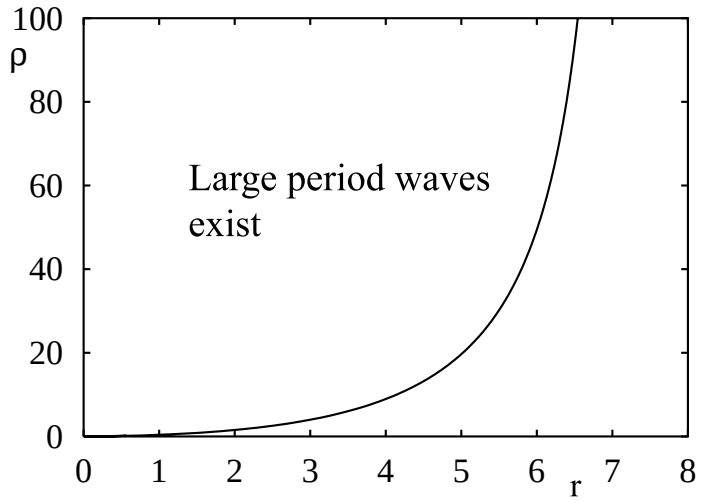

Fig. 6. Periodic waves of large period ($\Delta \to \infty$) exist to the left of the solid line in the (r, ρ) parameter plane. Parameters are $g_L = 1.25$, $\eta_0 = 40$ and $\tau_R = 2$.

approximately constant velocity for a range of large periods and the vanishing of a solution for small periods, the reciprocal dispersion curve $c^{-1} = c^{-1}(\Delta)$ adopts an approximately exponential form (apart from where a supernormal wave occurs). This shape can be directly attributed to the inclusion of an absolute refractory period within the SDS model. In section 4 the exponential shape of the dispersion curve will be shown to play an important role in the generation of solutions which connect periodic spike trains. In the limit

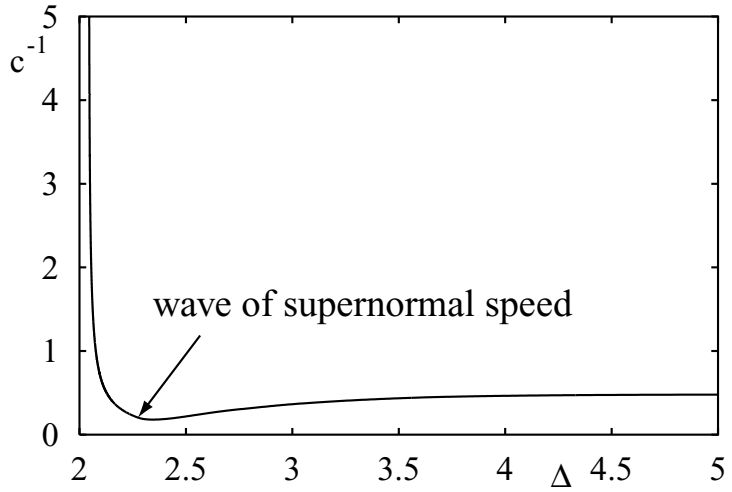

Fig. 7. The reciprocal of the travelling periodic wave speed as a function of the interspike interval Δ. Note that for large Δ we recover the speed of a stable solitary pulse. Parameters are $g_L = 1.25$, $r = 1$, $\rho = 25$, $\eta_0 = 40$ and $\tau_R = 2$.

$\Delta \to \infty$ the periodic wave becomes a solitary pulse. By taking the large Δ

limit of (21) we have that

$$1 = \frac{\sigma\lambda_-(1-\mathrm{e}^{-\lambda_+\tau_R})}{r(\widehat{\epsilon}+\lambda_+)} \tag{22}$$

where $\lambda_\pm = c_0[c_0 \pm \sqrt{c_0^2+4\epsilon}]/2$, and c_0 is the speed of the solitary wave, ie $c_0 = \lim_{\Delta\to\infty}(k\Delta)^{-1}$. Equation (22), defining the speed of a solitary wave, has previously been derived in [18], where a detailed discussion of the dependence of speed and stability upon system parameters can be found. In fact, in the limit as $\Delta \to \infty$, the branch of the reciprocal dispersion curve shown in figure 7 describes the *stable* solitary wave as determined by the analysis given in [18]. Another branch to the dispersion relation (21) also exists, but is associated with the slower unstable solitary travelling pulse (in the limit of large Δ) and so is expected to describe an unstable periodic travelling wave that would not be seen in numerical experiments like those of section 2.

3.1 Arbitrary pulse shape

The calculation of the dispersion curve for the SDS model is relatively straightforward for the case that the function $\eta(t)$ (describing the shape of a spine head action potential) is a rectangular pulse, since one only has to deal with a piecewise linear system of equations. The case of an arbitrary pulse shape cannot be analyzed in quite the same way. Here we develop a Green's function approach to deal with the general case.

The cable potential $V(x,t)$ satisfying equation (7) with the spine potential $\widehat{V}(x,t) = \sum_m \eta(t - T^m(x))$ can be evaluated in terms of the Green's function for the infinite cable equation as

$$V(x,t) = \frac{\rho}{r}\int_{-\infty}^{t} \mathrm{d}s \int_{-\infty}^{\infty} \mathrm{d}y G(x-y, t-s) \sum_m \eta(s - T^m(y)) \tag{23}$$

where

$$G(x,t) = \frac{1}{\sqrt{4\pi t}}\,\mathrm{e}^{-\epsilon t}\,\mathrm{e}^{-x^2/4t}\,\Theta(t) \tag{24}$$

If we now integrate (19) between two successive firing times and incorporate the reset condition, we obtain an implicit map of the firing times in the form

$$1 = \exp(-\widehat{\epsilon}[T^{n+1}(x) - T^n(x)] \int_{\tau_R}^{T^{n+1}(x)-T^n(x)} \mathrm{d}s\, \mathrm{e}^{\widehat{\epsilon}s}\, \frac{(V(x), s + T^n(x))}{r} \tag{25}$$

For a periodic travelling wave specified by the firing condition $T^n(x) = (n +$

$kx)\Delta$ equation (25) is equivalent to expression (20) with

$$V(t-x/c) = \frac{\rho}{r}\int_{-\infty}^{t} \mathrm{d}s \int_{-\infty}^{\infty} \mathrm{d}y G(x-y, t-s) F(s-y/c) \tag{26}$$

We can evaluate equation (26) by writing $F(s)$ as a Fourier series. That is, expand $F(s) = \sum_m a_m \, \mathrm{e}^{2\pi \mathrm{i} m s/\Delta}$ with $a_m = \widetilde{\eta}(2\pi m/\Delta)$, where

$$\widetilde{\eta}(p) = \sum_n \int_0^{\Delta} \eta(t - n\Delta)\, \mathrm{e}^{-\mathrm{i}pt}\, \mathrm{d}t = \int_{-\infty}^{\infty} \mathrm{d}t \eta(t)\, \mathrm{e}^{-\mathrm{i}pt} \tag{27}$$

and then perform the integrations over y and s in (26) with

$$\int_{-\infty}^{\infty} \mathrm{d}x\, \mathrm{e}^{-\mathrm{i}px}\, G(x,t) = \mathrm{e}^{-\epsilon(p)t}, \quad \epsilon(p) = \epsilon + p^2 \tag{28}$$

to obtain

$$V(x,t) = \frac{\rho}{r}\sum_m a_m \frac{\exp(2\pi \mathrm{i} m/\Delta(t - x/c))}{[\epsilon(2\pi m/\Delta c) + 2\pi \mathrm{i} m/\Delta]} \tag{29}$$

Hence, as expected, $V(x,t) = V(t-x/c)$ and is periodic in Δ. Note that we may also write $V(\xi)$ as a Fourier integral transform in the form

$$V(\xi) = \frac{\rho}{r}\sum_{m\in\mathbb{Z}} \int_{-\infty}^{\infty} \frac{\mathrm{d}p}{2\pi}\, \mathrm{e}^{\mathrm{i}p(\xi - m\Delta)}\, \frac{\widetilde{\eta}(p)}{\epsilon(p/c) + \mathrm{i}p} \tag{30}$$

Using the fact that $\eta(t) = 0$ for $t < 0$ it follows that any poles of $\widetilde{\eta}(p)$ lie in the upper-half complex plane so that we may restrict the sum in (30) to negative integer m. Using (20) and performing the sum over m in (30) we find that the dispersion relation for an arbitrary pulse shape is given implicitly as

$$1 = \frac{\rho}{r^2}\int_{-\infty}^{\infty} \frac{\mathrm{d}p}{2\pi} \frac{\widetilde{\eta}(p)}{(1 - \mathrm{e}^{ip\Delta})} \frac{\mathrm{e}^{\mathrm{i}p\Delta} - \mathrm{e}^{\mathrm{i}p\tau_R}\, \mathrm{e}^{\widehat{\epsilon}(\tau_R - \Delta)}}{(\epsilon(p/c) + \mathrm{i}p)(\widehat{\epsilon} + \mathrm{i}p)} \tag{31}$$

Note that for the rectangular pulse shape considered up till now

$$\widetilde{\eta}(p) = \eta_0 \frac{(1 - \mathrm{e}^{-\mathrm{i}p\tau_R})}{\mathrm{i}p} \tag{32}$$

It is straight forward to check using contour integration that for $\widetilde{\eta}(p)$ given by (32), (30) is equivalent to the solution previously given by other means as (15). In certain circumstances one might wish to include a decaying oscillatory tail in the shape of an action potential (say when the excitable spine head dynamics may be described with a set of nonlinear ordinary differential equations with a saddle-focus). In this case it is likely that the dispersion relationship will also be oscillatory, giving rise to the interesting possibility of multiple solutions of the same speed but differing period. For a discussion of this scenario in the spatially extended FHN model see [21,22].

4 A kinematic theory of spike trains

The stability of travelling waves in the SDS model may be analyzed in terms of the evolution of perturbations of the spine firing times. These perturbations evolve according to a nonlinear firing time map, which takes the form of an integro-difference equation of infinite order. As shown in previous work considerable simplification of this system of equations occurs in the long wavelength limit, relevant to the study of solitary pulses [18,23]. Here, we discuss a simplification of the underlying equations of motion for periodic travelling waves that sheds light not only on the conditions for stability in the full model but also allows a discussion of non-periodic travelling waves. In particular we highlight the ability of the SDS model to support connections between periodic spike trains, that can be associated with travelling wave fronts of the type observed numerically in section 2.

From the ansatz for periodic travelling waves we have that

$$\frac{\mathrm{d}T^n}{\mathrm{d}x} = \frac{1}{c} \tag{33}$$

where the speed of the wave $c = 1/(k\Delta)$. In fact, in the last section, we showed how to obtain $c = c(\Delta)$ for the SDS model. Previous success in formulating kinematic models of spike train dynamics has been obtained using (33) under the replacement $c \to c(T^n(x) - T^{n-1}(x))$, where $c(\Delta)$ is the dispersion relation for periodic travelling waves [21,20]. Since we have exactly the dispersion relation for periodic waves it is interesting to examine spike train dynamics within this so-called kinematic framework. First, let us consider a linear approximation for $c(\Delta)$ of the form

$$\frac{1}{c(\Delta)} = \frac{1}{c_0} - \gamma\Delta, \qquad \gamma = c_0'/c_0^2 \tag{34}$$

where c_0 is the speed of a solitary pulse. From figure 7 we would expect such an ansatz to hold in the long wavelength limit. In this case, the ISIs satisfy

$$\frac{\mathrm{d}\Delta_n}{\mathrm{d}x} = -\gamma[\Delta_n - \Delta_{n-1}], \qquad \Delta_n(x) = T^n(x) - T^{n-1}(x) \tag{35}$$

The general solution of (35) is given by

$$\Delta_n(x) = \sum_m G_{nm}(x)\Delta_m(0) \tag{36}$$

where

$$G_{nm}(x) = \mathrm{e}^{-\gamma x}[\mathrm{e}^{Kx}]_{nm}, \qquad K_{nm} = \gamma\delta_{n,m+1} \tag{37}$$

Using the series expansion for the matrix exponential $\exp(Kx)$ and noting that $[K^p]_{nm} = \gamma^p\delta_{n,m+p}$ (where $\delta_{n,m} = 1$ if $n = m$ and is zero otherwise) we

may write

$$G_{nm}(x) = \mathrm{e}^{-\gamma x} \sum_{p=0}^{\infty} \frac{x^p}{p!} [K^p]_{nm} = \mathrm{e}^{-\gamma x} \frac{(\gamma x)^{n-m}}{(n-m)!} \tag{38}$$

Hence,

$$\Delta_n(x) = \mathrm{e}^{-\gamma x} \sum_{p=0}^{n} \frac{(\gamma x)^p}{p!} \Delta_{n-p}(0) \tag{39}$$

For uniform initial data of the form $\Delta_n(0) = \Delta$ for all n we have that

$$\lim_{n\to\infty} \Delta_n(x) = \Delta \tag{40}$$

provided $\gamma > 0$. Hence, we may regard the condition $c_0' > 0$ as a weak form of linear stability for long wavelength periodic travelling waves (including solitary pulses). Note also that the solution for an initial spike train with a step sequence of the interspike intervals of the form $\Delta_n(0) = \Delta_{(1)}$, for $n < n^*$ and $\Delta_n(0) = \Delta_{(2)}$ for $n > n^*$ is given by

$$\Delta_n(x) = \Delta_{(1)} - (\Delta_{(1)} - \Delta_{(2)})\, \mathrm{e}^{-\gamma x} \sum_{p=0}^{n-n^*} \frac{(\gamma x)^p}{p!} \tag{41}$$

for large n^* ($n > n^*$). Hence, when $n - n^*$ is small the system at x fires repetitively with period $\Delta_{(1)}$, but as $n - n^*$ increases the period of oscillation changes to $\Delta_{(2)}$.

From our analysis of section 3, and in particular referring to figure 7, a better fit to $c(\tau)$ is given by

$$\frac{1}{c(\tau)} = \frac{1}{c_0} + A \exp(-B\tau) \tag{42}$$

For a succinct analysis of the firing times in the kinematic theory it is convenient to introduce a set of reference firing times in the form $T_r^n(x) = n\Delta_r + x/c(\Delta_r)$, for some arbitrary Δ_r. After a rescaling $T_n(x) \to B(T^n(x) - T_r^n(x))$ and $x \to AB \exp(-B\Delta_r)x$ we have that

$$\frac{\mathrm{d}T^n}{\mathrm{d}x} = \exp(-T^n(x) + T^{n-1}(x)) - 1 \tag{43}$$

where we choose Δ_r such that $[c_0^{-1} - c^{-1}(\Delta_r)] \exp(B\Delta_r)/A = -1$. With a further change of variables $z_n(x) = \exp T^n(x)$ we obtain an equation of the form (35) (with $\gamma = 1$), for which the general solution is given by (39). The solution for an initial spike train with a step sequence of the interspike intervals

is therefore

$$T^n(0) = \begin{cases} n\Delta_{(1)} & n \leq n^* \\ n^*\Delta_{(1)} + (n-n^*)\Delta_{(2)} & n > n^* \end{cases}$$

$$T^n(x) = \begin{cases} n\Delta_{(1)} + x/c(\Delta_{(1)}) & n \leq n^* \\ -x + \log\left\{\sum_{p=0}^{n-n^*} x^p/p! \exp[n^*\Delta_{(1)} + (n-n^*-p)\Delta_{(2)}]\right. & \\ \left. + \sum_{p=n-n^*}^{n} x^p/p! \exp[(n-p)\Delta_{(1)}]\right\} & n > n^* \end{cases} \tag{44}$$

A result of this form has previously been derived in [24] for the kinematic description of spikes in the spatially extended FHN model. Following [24], the steady state interspike intervals may be obtained using the above to construct $\Delta_n(x) = T^n(x) - T^{n-1}(x)$ and then examining the large n^* limit. Introducing $\omega = \Delta_{(2)} - \Delta_{(1)}$ and $\kappa = \exp(-\Delta_{(1)}) - \exp(-\Delta_{(2)})$ (assuming $\Delta_{(2)} > \Delta_{(1)}$) and letting $n \to n - n^*$ we have that

$$\Delta_n(x) = -\log\left(\exp(-\Delta_{(1)}) + \frac{\exp(-\Delta_{(2)}) - \exp(-\Delta_{(1)})}{1 + \exp(\kappa x - \omega n)}\right) \tag{45}$$

Note that this sequence is a function of $z = \kappa x - \omega n$ such that $\Delta_n(x) = \Delta(z)$. It is clear that $\Delta(z) \to \Delta_{(1)}$ as $z \to \infty$ and $\Delta(z) \to \Delta_{(2)}$ as $z \to -\infty$. Hence, solutions may be regarded as connections to periodic spike trains of interspike intervals $\Delta_{(1)}$ and $\Delta_{(2)}$. Moreover, the position of the front connecting the two periodic orbits moves with a constant group velocity $\mathrm{d}n/\mathrm{d}\omega = \kappa/\omega$. The front moves backwards for $\Delta_{(2)} > \Delta_{(1)}$ and forwards for $\Delta_{(1)} > \Delta_{(2)}$. In figure 8 we show a plot of the sequence of ISIs given by (45). Note the similarity of the shape of the propagating front to that shown in figure 4 for the numerical simulation of the Baer and Rinzel model.

4.1 Stability of non-uniform finite spike trains

A steadily propagating general wavetrain is stable if under the perturbation $T^n(x) \to T^n(x) + u^n(x)$ the system converges to the unperturbed solution during propagation, or $u^n(x) \to 0$ as $x \to \infty$. For the case of uniformly propagating periodic travelling waves of period Δ we insert the perturbed solution in (33), so that to first order in the u^n

$$\frac{\mathrm{d}u^n}{\mathrm{d}x} = -\frac{c'(\Delta)}{c^2(\Delta)}[u^n - u^{n-1}] \tag{46}$$

Thus, a uniformly spaced, infinite wavetrain with period Δ is stable (within the kinematic approximation) if and only if $c'(\Delta) > 0$. For the dispersion curve shown in figure 7 $c'(\Delta) > 0$ everywhere except when the speed of the

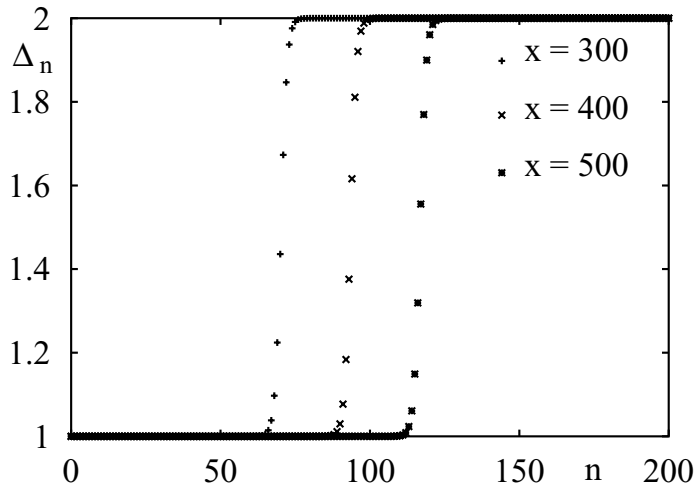

Fig. 8. A graphical illustration of the travelling front obtained analytically from the kinematic description of the SDS model. Initial data at $x = 0$ is a step sequence in the interspike intervals with $\Delta_{(1)} = 1$ and $\Delta_{(2)} = 2$.

wave is supernormal. Of the two possible supernormal waves only the one with $c'(\Delta) > 0$ is expected to be stable. The kinematic analysis also predicts that of the two possible waves of large period ($\Delta \to \infty$) it is the fastest that is stable. This is consistent with the result in [18] for the stability of solitary pulses. We now consider the stability of finite non-uniform trains, rather than the more involved case of general trains of infinite extent. This allows us to make the realistic assumption that the speed of the leading pulse is c_0 (the speed of a solitary pulse) so that we may write $T^n(x) = x/c_0 + \sum_{k=1}^{n} \Delta_n$, $n = 1, \ldots, N$ [22]. Proceeding as before we find the linear equations

$$\frac{\mathrm{d}u^1}{\mathrm{d}x} = 0, \qquad \frac{\mathrm{d}u^n}{\mathrm{d}x} = \frac{c'(\Delta_n)}{c^2(\Delta_n)}[u^n - u^{n-1}], \qquad n = 2, \ldots, N \tag{47}$$

Thus a non-uniform train is stable if and only if $c'(\Delta_n) > 0$ for each n (ignoring the zero eigenvalue associated with translations of the leading pulse). Since the solutions describing connections between periodic orbits are constructed from a dispersion curve with $c'(\Delta) > 0$ for all realisable Δ, we expect them to be stable.

5 Discussion

Numerical simulations of the Baer and Rinzel model, for the description of dendritic tissue with active spines, have been used to demonstrate the existence of both periodic travelling waves and waves which connect periodic orbits for initial data in the form of a spike train with a step change in the interspike

interval. The spike-diffuse-spike model was shown analytically to support the same type of behavior, supporting the claim that is a useful caricature of the more complex Baer and Rinzel model. It would appear that when travelling waves, fronts and pulses are concerned, integrate-and-fire models yield similar qualitative behaviour as conductance based models. This conclusion has also been drawn in the work of Golomb and Ermentrout on propagating pulses in cortical and thalamic neuronal networks [25]. The fact that wave fronts (in the sequence of ISIs of the spike-diffuse-spike model) can propagate with an invariant shape at constant speed can be traced to the (analytically determined) exponential shape of the dispersion relationship for periodic waves and hence to the refractoriness of the spine head dynamics. Hence, (at least for uniform unbranched pieces of dendrite with a constant continuous distribution of spines) signals encoded in dendritic waves might be transmitted without degrading edge pattern.

Of course, in a real neuron one might expect scattering of electrical waves from branch points where there is some impedance mismatch between parent and daughter dendrites. For an analytic study one might consider individual segments of a branching structure that consist of finite pieces of cable with SDS dynamics and a branching structure prescribed by some graph with boundary conditions at branch points determined by Kirchoff's laws. The use of techniques for the description of *echo-waves* in nonuniform excitable fibers may also be appropriate [26]. As well as studying more realistic neuronal geometries it is of interest to move away from the description of the spine neck as a lumped ohmic resistor. For instance, it is known that the spine neck can transport Ca^{2+} from the spine head to the dendritic shaft and that it can function as a Hebbian synapse or weight [10]. By considering the spine stem resistance as an activity dependent synaptic weight Wu and Baer [11] have demonstrated the fascinating possibility of spines being able to generate complex oscillatory behavior including bursting. The effect of spine adaptation within the SDS model is another natural extension of the work in this paper. It is hoped that further mathematical analysis of these extensions to the SDS model will increase our understanding of the role of dendritic spines in real time signal processing within the central nervous system.

Acknowledgments

The work in this paper was supported in part by a grant from the Nuffield Foundation in the form of an award to newly appointed lecturers in Mathematics.

Appendix A

For the Hodgkin-Huxley model of excitable nerve tissue it is common practice to write

$$\tau_X(V) = \frac{1}{\alpha_X(V) + \beta_X(V)}, \qquad X_\infty(V) = \alpha_X(V)\tau_X(V)$$

for $X \in \{m, n, h\}$ where

$$\alpha_m(V) = \frac{0.1(V+40)}{1-\exp[-0.1(V+40)]} \qquad \beta_m(V) = 4.0\exp[-0.0556(V+65)]$$
$$\alpha_h(V) = 0.07\exp[-0.05(V+65)] \qquad \beta_h(V) = \frac{1}{1+\exp[-0.1(V+35)]}$$
$$\alpha_n(V) = \frac{0.01(V+55)}{1-\exp[-0.1(V+55)]} \qquad \beta_n(V) = 0.125\exp[-0.0125(V+65)]$$

All potentials are measured in mV, all times in ms and all currents in μA per cm^2. The following parameter values are used in numerical simulations: $C = 1\mu$F cm^{-2}, $g_L = 0.3$mmho cm^{-2}, $g_K = 36$mmho cm^{-2}, $g_{Na} = 120$mmho cm^{-2}, $V_L = -54.402$mV, $V_K = -77$mV and $V_{Na} = 50$mV.

References

[1] R G Coss. The function of dendritic spines: a review of theoretical issues. *Behaviorial and Neural Biology*, 44:151–185, 1985.

[2] E G Gray. Axo-somatic and axo-dendritic synapses of the cerebral cortex: an electron microscopic study. *Journal of Anatomy*, 93:420–433, 1959.

[3] I Segev and W Rall. Excitable dendrites and spines: earlier theoretical insights elucidate recent direct observations. *Trends in Neuroscience*, 21(11):453–460, 1998.

[4] M Barinaga. Spines shed their dull image. *Science*, 268:200–201, 1995.

[5] R Yuste and W Denk. Dendritic spines as basic functional units of neuronal integration. *Nature*, 375:682–684, 1995.

[6] C Koch, A Zador, and T H Brown. Dendritic spines: convergence of theory and experiment. *Science*, 256:973–974, 1992.

[7] K M Harris and S B Kater. Dendritic spines: cellular specializations imparting both stability and flexibility to synaptic function. *Annual Review of Neuroscience*, 17:341–371, 1994.

[8] I Segev and W Rall. Computational study of an excitable dendritic spine. *Journal of Neurophysiology*, 60(2):499–523, 1988.

[9] N Qian and T J Sejnowski. An electro-diffusion model for computing membrane potentials and ionic concentrations in branching dendrites, spines and axons. *Biological Cybernetics*, 62:1–15, 1989.

[10] A Zador, C Koch, and T H Brown. Biophysical model of a Hebbian synapse. *Proceedings of the National Academy of Sciences USA*, 87:6718–6722, 1990.

[11] H Y Wu and S M Baer. Analysis of an excitable dendritic spine with an activity-dependent stem conductance. *Journal of Mathematical Biology*, 36:569–592, 1998.

[12] J P Miller, W Rall, and J Rinzel. Synaptic amplification by active membrane in dendritic spines. *Brain Research*, 325:325–330, 1985.

[13] D H Perkel and D J Perkel. Dendritic spines: role of active membrane in modulating synaptic efficacy. *Brain Research*, 325:331–335, 1985.

[14] G M Shepherd, R K Brayton, J P Miller, I Segev, J Rinzel, and W Rall. Signal enhancement in distal cortical dendrites by means of interactions between active dendritic spines. *Proceedings of the National Academy of Sciences USA*, 82:2192–2195, 1985.

[15] W Rall and J Rinzel. Dendritic spine function and synaptic attenuation calculations. *Progam and Abstracts Society for Neuroscience*, 1:64 (7C), 1971.

[16] G J Rose and S J Call. Evidence for the role of dendritic spines in the temporal filtering properties of neurons: The decoding problem and beyond. *Proceedings of the National Academy of Sciences USA*, 89:9662–9665, 1992.

[17] S M Baer and J Rinzel. Propagation of dendritic spines mediated by excitable spines: A continuum theory. *Journal of Neurophysiology*, 65(4):874–890, 1991.

[18] S Coombes and P C Bressloff. Solitary waves in a model of dendritic cable with active spines. *SIAM Journal on Applied Mathematics*, 61:432–453, 2000.

[19] Y Zhou. Unique wave front for dendritic spines with Nagumo dynamics. *Mathematical Biosciences*, 148:205–225, 1998.

[20] R N Miller and J Rinzel. The dependence of impulse propagation speed on firing frequency, dispersion, for the Hodgkin-Huxley model. *Biophysical Journal*, 34:227–259, 1981.

[21] J Rinzel and K Maginu. Kinematic analysis of wave pattern formation in excitable media. In C Vidal and A Pacault, editors, *Non-Equilibrium Dynamics in Chemical systems*, pages 107–113. Springer-Verlag, 1984.

[22] C Elphick, E Meron, J Rinzel, and E A Spiegel. Impulse patterning and relaxational propagation in excitable media. *Journal of Theoretical Biology*, 146:249–268, 1990.

[23] P C Bressloff. Traveling waves and pulses in a one-dimensional network of excitable integrate-and-fire neurons. *Journal of Mathematical Biology*, 40:169–198, 1999.

[24] Y Horikawa. A spike train with a step change in the interspike intervals in the FitzHugh-Nagumo model. *Physica D*, 82:365–370, 1995.

[25] D Golomb and G B Ermentrout. Continuous and lurching traveling pulses in neuronal networks with delay and spatially decaying activity. *Proceedings of the National Academy of Sciences USA*, 96:480–485, 1999.

[26] Y Zhou and J Bell. Study of propagation along nonuniform excitable fibers. *Mathematical Biosciences*, 119:169–203, 1994.